Astron. Astrophys. 349, 276–282 (1999)

ASTRONOMY
AND
ASTROPHYSICS

Radial velocities of optical lines in three bright Galactic HII regions⋆

César Esteban[1] **and Manuel Peimbert**[2]

[1] Instituto de Astrofísica de Canarias, E-38200 La Laguna, Tenerife, Canary Islands, Spain (cel@ll.iac.es)
[2] Instituto de Astronomía, UNAM Apdo. Postal 70–264, Mexico D.F. 04510, Mexico (peimbert@astroscu.unam.mx)

Received 31 March 1999 / Accepted 11 May 1999

Abstract. We present heliocentric radial velocities for a large number of emission lines covering all the optical spectral range for two slit positions of the Galactic H II regions M 42 and M 17 and one slit position of M 8. We obtain a fairly similar relation between the heliocentric velocity and the ionization potential of the ions in all the observed slit positions. This general result indicates a similar behaviour of the velocity stratification along the line of sight in the three objects. We suggest that flows of ionized gas streaming away from the molecular clouds toward the observer can explain qualitatively the observations.

Key words: ISM: H II regions – ISM: individual objects: M 17 – ISM: individual objects: M 42 – ISM: individual objects: M 8 – ISM: kinematics and dynamics

1. Introduction

Kinematic studies are powerful tools to understand the structure of H II regions and the dynamics involved in their evolution. Of special interest is the investigation of the radial velocity of the emission lines produced by ions with different ionization potential. This information could give important insights into the spatial velocity stratification in a given line of sight inside the nebula. The first paper devoted to this kind of study for a Galactic H II region was that by Kaler (1967), who presented radial mean velocities from emission lines of a variety of ions taken from photographic spectra of the Orion nebula (M 42) published by Kaler et al. (1965). This author found a distinct relation between ionization potential of the ions producing the observed emission lines and their radial velocity, in the sense that the ions with higher ionization potential present more negative radial velocities. A similar but more restricted result was obtained previously by Wilson et al. (1959) from observations of [O II] and [O III] lines. The velocity-ionization potential relation found by Kaler shows a sharp change in velocities (of about 10–15 km s^{-1}) between the lines of high ionization potential ions (such as S^{3+}, O^{++} and Ne^{++}) and those produced by low ionization potential ones (such as Fe^{+} and Fe^{++}). Moreover, Fehrenbach (1977) reported additional measurements including emission lines for more ions in two zones of M 42, finding a similar velocity stratification.

The most recent, detailed and extensive kinematic studies of M 42 have been carried out in several papers by O'Dell, Wen and Castañeda. In particular, Castañeda (1988) presented the analysis of the profile of the [O II] line in 900 different positions; O'Dell & Wen (1992) measured the radial velocities of the [O I] line; and Wen & O'Dell (1993) performed a kinematic study of the [S III] emission. O'Dell & Wen (1992) in their Table 5, give the mean value of the heliocentric velocities of the [O I], [S II], [N II], [O II], H I, [O III], and [S III] lines finding that although there exist differences between the velocities of [O I] and [S II] with respect to the others, the rest of the ions present quite similar radial velocities. It is remarkable that the heliocentric velocity of [O I] is very similar to the mean heliocentric velocity of the molecules in the OMC-1 cloud core (see Goudis 1982, and references therein). This fact, and the presence of the aforementioned velocity-ionization potential relation, led O'Dell & Wen (1992) to propose the presence of flows of freshly ionized gas from the ionization front to the fully ionized zone. This interpretation was firstly outlined by Zuckerman (1973) and Balick et al. (1974); they assumed that the ionization front is behind the Trapezium, between the molecular cloud and the H II region, and that the H II region is density bounded in the direction to the observer.

Very recently, the similarity between the heliocentric velocity of [O I] and [Fe II] and that of OMC-1 has been considered by Bautista & Pradhan (1998) as one of the evidences to argue that both line emissions are produced at the partially ionized zone of M 42. This result has important consequences on the conditions where the [Fe II] spectrum is produced, a controversial subject in recent years (see Bautista & Pradhan 1995, 1998; Baldwin et al. 1996; Esteban et al. 1999a).

The kinematic studies of M 8 and M 17 are not so extensive and detailed as those of M 42, however a relatively large amount of information is available for both objects. For M 8 Elliott & Meaburn (1975a) performed an analysis of the [O III] line profile in many positions covering a large area of the nebula. These authors found splittings (firstly reported by Dopita 1972) with radial velocity differences of up to +18 km s^{-1} in large zones of the core of M 8 and associated with the dark neutral intrusions.

Send offprint requests to: C. Esteban

⋆ Based on data obtained at the Observatorio Astronómico Nacional, SPM, B.C., Mexico

These kinematic features could be explained by the presence of two separate flows of ionized gas from two separate ionization fronts along the line of sight to the core of M 8. On the other hand, Elliott et al. (1984), from the study of absorption Na I lines and [O III] and [N II] emission lines over a large area of M 8, suggested that the observed line splitting could be due to the action of a bipolar shell produced by the stellar wind of the ionizing star H 36 expanding over a highly non-uniform ambient. Finally, Hänel (1987) obtained Fabry-Pérot observations for Hα, [S II], [N II] and [O III] over the whole nebula. The complexity of the velocity fields detected, as well the similarities between CO brightness maps and the kinematics of the emission lines, lead Hänel (1987) to interpret the observed motions in M 8 as the result of flows of ionized gas away from the ionization fronts. As in the case of M 42, Hänel (1987) obtained for M 8 that lines from higher ionization gas have blueshifted velocities with respect to those of lower ionization gas and the molecular cloud.

Line splitting was observed firstly by Elliott & Meaburn (1975b) in M 17. Goudis & Meaburn (1976) obtained Fabry-Pérot [O III] observations covering almost the whole nebula and compared the radial velocities with those observed for the molecular and neutral material. These authors found, that the most complex [O III] profiles are present near the dark neutral zones, as in the case of M 8. Elliott et al. (1978) confirmed the previous results of Goudis & Meaburn (1976) from the analysis of [O III] and [N II] line profiles and support the model proposed by Meaburn (1977), which interprets M 17 as composed of a series of partial shells which are neutral on their outsides and ionized on their inside surfaces. In this model, the shells are assumed to be expanding due to the action of the stellar winds. On the other hand, Meaburn & Walsh (1981) identified very faint high-velocity features in M 17 with velocities of the order of 180 km s^{-1}. They discuss the different mechanisms for the formation of the high-velocity phenomena (basically flows from ionization fronts and effects of stellar winds) concluding that probably all the mechanisms are contributing in various proportions. Clayton et al. (1985) reach the same conclusion, but favouring the presence of expanding shells due to the action of wind-driven bubbles as the most likely origin of the complex kinematics of M 17.

In this paper we present a homogeneous set of echelle observations in one or two slit positions of three of the bightest H II regions: M 42, M 8 and M 17. The observations cover a large number of emission lines of many different ions from optical to near-infrared wavelengths. In contrast with previous similar studies as those of Kaler (1967) and Fehrenbach (1977) for M 42 (which were based on photographic plates) the present observations are based on CCD spectra.

2. Observations

The observational data presented in this paper are based on the reanalysis of the echelle spectra published previously for M 42 (Esteban et al. 1998), M 8 (Esteban et al. 1999b) and M 17 (Esteban et al. 1999c).

All the observations were carried out with the 2.1-m telescope of the Observatorio Astronómico Nacional at San Pedro Mártir, Baja California, Mexico, on different observing runs from 1994 to 1996. The high resolution spectra were obtained using the REOSC Echelle Spectrograph in its cross-dispersing mode. This instrument gives a resolution of 0.234 Å pixel^{-1} at Hα using a CCD-Tek chip of 1024 $\times$ 1024 pixels with a 24 μm^2 pixels size. The spectral resolution is of 0.5 Å FWHM and the accuracy in the wavelength determination of emission lines is about 1–1.5 km s^{-1} depending on the wavelength of the emission line. Slits covering 13.3″$\times$2″ in the blue exposures (3500–5800 Å), 26.6″$\times$2″ in the red ones (4600–7060 Å) and 39.9″$\times$2″ in both near-infrared (NIR) exposures were used to avoid overlapping between orders. We have taken one slit position for M 8 and two for M 42 and M 17. In all cases the position angle was east-west. Typically, three or four individual exposures were added to obtain the final spectra in each range. In some cases, we took additional short time exposures to have good measurements of the brightest lines and avoid problems of saturation. We used a Th-Ar lamp for wavelength calibration of all spectra. A journal of observations is presented in Table 1.

A more detailed description of the observations and data reduction can be found in Esteban et al. (1998, 1999b, and 1999c).

3. Line profile analysis

Accurate measurement of the central wavelength of the emission lines was obtained via Gaussian fitting of the profiles. As a general result, all the emission lines not affected by line-blending are well reproduced with a single Gaussian fit (i.e. no line-splitting is reported at our resolution limit). The fitting was performed with the SPLOT routine of the IRAF[1] reduction package. We have extended the kinematic analysis to the largest number of emission lines attending to these criteria:

- We select only those lines showing a clear single profile (i.e. not affected by line-blending) or those blended but resolved enough to perform an accurate double Gaussian fitting.
- We have included only those lines whose excitation mechanism is well known. Specially, in M 42 and M 8 there is a large number of permitted lines of heavy elements whose main excitation mechanism should be line or stellar continuum fluorescence. In these cases, we do not know the exact percentage of the contribution due to recombination and fluorescence to the line strength (the contribution of each of these two types of lines is representative of different ionization stages of the element), therefore they have not been considered. The final list includes: H I and He I recombination lines; forbidden lines; permitted lines of heavy elements which are produced largely by recombination [see detailed discussion on excitation mechanisms in Esteban et al. (1998) and Esteban et al. (1999b)].

[1] IRAF is distributed by NOAO, which is operated by AURA, Inc., under contract with the NSF.

Table 1. Journal of observations

Nebula	Zone	Date	$\Delta\lambda$ (Å)	orders	Exp. Time (s)	Location
M 42	Position 1	94/10/28	4500–6850	49–33	120, 4800	45″N of θ^1 Ori C
		95/3/26	3550–5800	62–39	300, 3600	
	Position 2	95/3/25	4600–7060	48–32	120, 3600	25″S and 10″W
		95/3/26	3550–5800	62–39	300, 3600	of θ^1 Ori C
M 8	HGS	95/8/24	3500–5950	38–63	600, 3600	25″S of center of HG
		95/8/23	4600–7075	30–46	60, 4800	
		96/6/10	6450–9100	25–34	60, 3600	
		96/6/13	8450–10300	22–26	2700	
M 17	Position 3	95/8/22	3500–5950	38–63	3600	250″S and 54″W
		95/8/23	4600–7075	30–46	300, 4800	of BD−16°4819
		96/6/10	6450–9100	25–34	300, 3600	
		96/6/13	8450–10300	22–26	1800	
	Position 14	95/8/24	3500–5950	38–63	3600	300″S and 72″E
		96/6/11	6450–9100	25–34	300, 2700	of BD−16°4819
		96/6/13	8450–10300	22–26	2100	

– We have not considered lines located near (about 30 or 40 Å) the edges of the spectral orders due to the usual inaccurate wavelength calibration in these regions.
– For most lines, our set of data permits to have several different measurements of the same line. This is because we have overlapping zones in the consecutive spectral orders and the different spectral intervals covered with wide common regions. In these cases, we have adopted the mean value of the central wavelength given by the different measurements available for each line.

4. Results and discussion

In Table 2 we present the heliocentric velocity adopted for each ion and for each slit position observed in the three nebulae. The values given in the table correspond to the mean of the velocities measured for all the individual lines useful for each ion. The number of lines considered to calculate this average is indicated in brackets after the velocity. The uncertainty associated with each velocity includes the standard deviation of the average and the accuracy of the wavelength determination. In this table we present heliocentric velocities for an unprecedently large number of ionic species (between 12 and 17, depending on the slit position and object) in the same line of sight of H II regions, even for M 42, the most studied of the objects included in this paper. The range of ionization potential covered goes from neutral species as O I and N I to Ne III (41 eV). The emission lines of the heavy elements used are mainly collisionally excited ones except in the case of the single line of C^{++} used (C II λ 4267 Å) and the O II recombination lines which have been used in combination with the [O III] lines to derive the mean value included in Table 2. For O III, the velocities obtained from individual permitted and collisionally excited lines are in complete agreement.

In Fig. 1 we present the observed average heliocentric velocities of the ions vs. the minimum photon energy required to produce the ionized species for the different slit positions observed in M 42, M 8 and M 17. These diagrams are adapted from similar ones constructed for M 42 by Kaler (1967), Balick et al. (1974) and Bautista & Pradhan (1998). The velocity of the associated molecular clouds is indicated by a dashed horizontal line for each H II region.

For the two slit positions observed in M 42, we can see a clear dependence of the heliocentric velocity of the ions and their formation energy. As it was stated in Sect. 1, this behaviour was reported previously by Kaler (1967) and Fehrenbach (1977). However, in our case we have data for more ions, covering more densely the range of photon energies available. In the case of Position 2, there is an apparent smooth and continuous decrease of the heliocentric velocity along all the range of ionization potential. The difference in velocity between the lines of neutral species and those of [Ar IV] and [Ne III] is about 15 km s^{-1}. In the case of Position 1, there is a relatively sharp change in velocity between neutral species and Fe II and the rest of the ions, in fact, the heliocentric velocity seems to be rather constant from S II to Ne III ($v_{hel} \approx 21$ km s^{-1}) within the uncertainties except in the case of the single line of [Ar IV] observed, which is 11 km s^{-1} lower. In average, the change in velocity between the neutral species and Fe II and the rest of the ions is about 6 km s^{-1}.

In Table 3 we compare the heliocentric velocities that we obtain for our Positions 1 and 2 of M 42 with those by O'Dell & Wen (1992), Kaler (1967) and Fehrenbach (1977) for the ions in common. It can be seen that there is in general a good agreement, even taking into account that the zones observed are not exactly the same and that the data of O'Dell & Wen (1992) correspond to average values over a large fraction of the surface of M 42. The behaviour of the velocity-ionization potential relation obtained by O'Dell & Wen (1992) is similar to the one obtained for our Position 1, with a sharp change in velocity between high and low ionization energy ions and a constant velocity for the highly ionized species. On the other hand, the

Table 2. Heliocentric velocities of ions in M 42, M 8 and M 17 (in km s^{-1})$^{(1)}$

	I.P.	M 42		M 8	M 17	
Ion	(eV)	Position 1	Position 2	HGS	Position 3	Position 14
N^0	0	26.3±1.4 (2)	26.8±1.4 (2)	−7.2±1.4 (2)	10.4±3.4 (2)	8.6±1.6 (2)
O^0	0	26.8±1.6 (2)	24.6±2.2 (2)	−14.0±1.8 (2)	2.3±7.4 (2)	...
Ni^+	7.6	...	...	2.0±1.0 (1)	...	...
Fe^+	7.9	27.8±5.1 (11)	29.4±5.6 (12)	−5.8±3.1 (7)	...	...
S^+	10.4	22.0±1.8 (3)	23.2±2.3 (3)	−3.5±3.6 (4)	10.9±1.4 (2)	6.7±1.8 (3)
Cl^+	13.0	...	...	...	6.3±2.1 (1)	...
H^+	13.6	20.4±3.2 (17)	14.0±2.0 (15)	−0.2±6.6 (48)	2.1±5.3 (35)	0.3±4.3 (37)
O^+	13.6	19.7±2.9 (2)	21.3±2.8 (2)	−0.5±2.9 (4)	5.6±2.2 (2)	−2.8±3.4 (2)
N^+	14.5	19.7±2.8 (4)	20.0±3.9 (4)	−2.0±4.5 (4)	9.1±5.3 (3)	2.8±4.2 (4)
Fe^{++}	16.2	19.5±4.3 (15)	23.0±4.7 (14)	−1.9±3.5 (15)	4.8±4.5 (4)	−1.9±5.2 (5)
S^{++}	23.3	17.6±1.3 (1)	19.0±1.3 (1)	−0.5±1.3 (1)	4.8±1.1 (1)	...
Cl^{++}	23.8	15.5±2.3 (2)	12.5±2.0 (2)	−6.2±1.2 (2)	3.8±1.5 (2)	−0.5±2.3 (2)
C^{++}	24.4	21.1±1.5 (1)	13.4±1.5 (1)	−4.2±1.5 (1)	0.0±1.5 (1)	1.41±1.5 (1)
He^+	24.6	19.3±2.7 (20)	14.0±3.0 (19)	−5.1±2.9 (22)	−1.4±4.2 (18)	−2.0±4.4 (29)
Ar^{++}	27.6	9.8±1.4 (1)	6.4±1.4 (1)	−6.8±5.2 (3)	0.0±6.6 (3)	1.1±2.9 (3)
O^{++}	35.1	17.6±3.1 (23)	9.9±6.0 (16)	−7.5±3.1 (15)	0.9±2.8 (7)	0.6±5.4 (8)
Cl^{3+}	39.6	...	...	...	−7.5±1.0 (1)	...
Ar^{3+}	40.7	18.1±4.0 (2)	11.1±1.6 (2)	...	0.0±1.5 (1)	...
Ne^{++}	41.0	22.5±2.2 (2)	11.1±1.9 (2)	−13.4±2.6 (2)	−3.1±1.8 (2)	−5.0±2.8 (2)

$^{(1)}$ The number of individual lines averaged to obtain each given velocity is in brackets.

Table 3. Comparison with previous velocity determinations for M 42 (in km s^{-1})

	This work				
Ion	Position 1	Position 2	O'Dell & Wen (1992)	Kaler (1967)	Fehrenbach (1977)
O^0	26.8±1.6	24.6±2.2	25.8	...	...
Ni^+	...	...	...	...	27.8
Fe^+	27.8±5.1	29.4±5.6	...	26.9±0.8	24.2
S^+	22.0±1.8	23.2±2.3	21.6	...	...
H^+	20.4±3.2	14.0±2.0	15.5	20.1±0.25	14.2
O^+	19.7±2.9	21.3±2.8	13.8	...	14.7
N^+	19.7±2.8	20.0±3.9	19.1	...	...
Fe^{++}	19.5±4.3	23.0±4.7	...	27.4±0.6	15.2
S^{++}	17.6±1.3	19.0±1.3	10.7	...	...
O^{++}	17.6±3.1	9.9±6.0	15.4	17.3±1.4	14.0
Ne^{++}	22.5±2.2	11.1±1.9	...	13.9±2.0	13.5

behaviour of the gradient reported by Kaler (1967) is similar to that obtained for our Position 2, reaching similar blueshifted velocities for Ne III. Unfortunately, Kaler et al. (1965) do not give a precise indication about their observing zone. They only indicate that their spectrum was taken on the "brightest zone of the nebula", which probably correspond either to the west or south-west of the Trapezium (in this case it should include our Position 2 or zones close to it) or to the "Orion bar" zone. Finally, Fehrenbach (1977), who presents average values for two different regions, obtains a relation quite similar to our Position 1 and that of O'Dell & Wen (1992), with a clear change of the heliocentric velocity between ions with lower and higher ionization potentials with respect of S II.

Figs. 1a and 1b show also that the heliocentric velocities of the neutral species (O I and N I) and of Fe II coincide, within the uncertainties, with that of the molecules in OMC-1 (see Goudis 1982, and references therein), the molecular cloud associated to M 42. This fact was already pointed out by Bautista & Pradhan (1998) and interpreted as an evidence that the [Fe II] is produced at the partially ionized zone of M 42. This possibility is confirmed in our data for both slit positions.

In Fig. 1c we show the velocity-ionization potential relation for the southern part of the Hourglass (HGS) zone in M 8, which shows a relatively complex behaviour due to the peaked distribution of the velocities at energies close to the ionization of Hydrogen. At these energies, the velocity of the different ionic species is similar to that of the associated molecular cloud in the zone adjacent to HGS, $v_{hel} \approx -1$ km s^{-1} (Lada et al. 1976; Wright et al. 1977). Also in Fig. 1c, it can be seen that the heliocentric velocity of the lines becomes more negative for both higher ionization potential ions and neutral species. This behaviour of lower heliocentric velocities for the higher excited

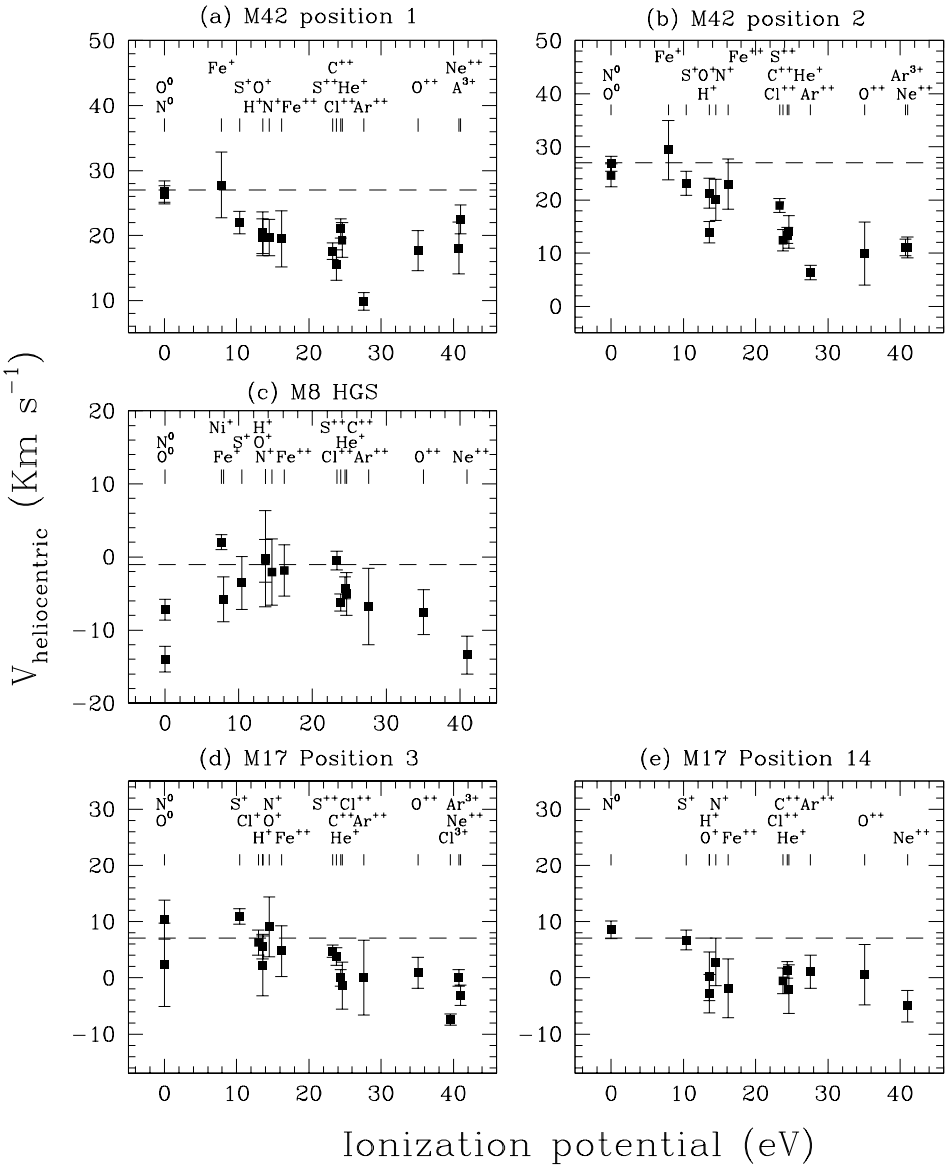

Fig. 1a–e. Heliocentric velocities of emission lines in the different slit positions observed vs. the minimum photon energy required to produce the ionized species. The velocity of the associated molecular cloud is indicated by a dashed horizontal line. The relative positions of the different labels of the ions correspond roughly to the relative positions of the observational data below. The label above each box indicates the corresponding nebula and slit position.

ions is consistent with that found for the rest of the H II regions observed. In contrast, the velocities found for O I and N I in the HGS zone of M 8 are discrepant one with each other, with the general trend of the rest of the ions and with the velocity of the molecular cloud. The profiles of the O I and N I lines do not show apparent line-splitting. However, this difference, at least for O I, could be explained by a slight contamination of the line profiles either by sky emission or other nebular kinematic components. In fact, the full width at half maximum (FWHM) of the [O I] lines is about a factor 25% larger than for the rest of the neighbouring forbidden lines. In this sense, it is important to comment that the presence of several kinematic components in the core of M 8 has been reported for both ionized and neutral gas in previous works with higher spectral resolution (e.g. Elliott & Meaburn 1975a; Elliott et al. 1984). Components with heliocentric velocities of the order of -8 to $-14\,\mathrm{km\,s^{-1}}$ are common in this nebula (Elliott et al. 1984). However, the fact that this hypothetical second component is detected only in the neutral species would imply that this feature has very different an unusual ionization conditions.

In Figs. 1d and 1e we show the velocity-ionization potential relation for the two slit positions observed of M 17. As in the other H II regions, the heliocentric velocity becomes lower as the ionization potential of the ions increases. In the case of Position 3, the average velocity of the ions with potentials around 13.6 eV is very similar to that of the molecular cloud M 17SW ($v_{hel} \approx 7\,\mathrm{km\,s^{-1}}$, Lada, Dickinson, & Penfield (1974) but, in contrast, in Position 14, the velocities of this group of ions are almost $10\,\mathrm{km\,s^{-1}}$ lower. On the other hand, in both slit positions, the heliocentric velocity of the neutral species are similar to that of the molecular cloud, a result obtained also for M 42. Position 3 shows a smoothly decreasing behaviour of the velocity-ionization potential distribution, which is similar to that of Position 2 of M 42 and M 8 (excluding the neutral species in this last case). In contrast, Position 14 shows (similarly to Position 1 of M 42) a change between the velocity of the

low energy ions (N I and S II) and the rest of them, which have a mean velocity of$v_{hel} \approx -1$ km s^{-1}, about 8 km s^{-1} lower than the velocity of the associated molecular cloud.

We consider that the most important result of this work is the finding of a qualitatively similar behaviour of the velocity-ionization potential relation of the ions in all the H II regions observed. This indicates that the spatial stratification of the velocities of the ionized gas in this three objects is similar and, probably, produced by a similar physical process.

The picture of flows of ionized gas streaming away from the molecular cloud towards the observer seems to be the most suitable scenario to explain the basic observational features reported, as the general decrease of the heliocentric velocity with the ionization energy, and the similarity of the velocity of the neutral species with that of the associated molecular clouds (found in the case of M 42 and M 17). In this scenario (e.g. Zuckerman 1973; Balick et al. 1974; O'Dell & Wen 1992), the neutral species and lower ionized gas close to the ionization front are still at rest or moving into the molecular cloud, while higher excited gas closer to the ionizing star is moving away from the neutral gas with velocities up to the speed of sound. In fact, the differences in velocity between the neutral material and the high ionized species are of 6–15 km s^{-1} in all cases, of the order of the typical sound speed in ionized nebulae. Another observational fact, that could be easily explained by this scenario, is the systematic negative velocity differences between low and high ionized species. This could simply be due to the fact that we can only see those H II regions which are located in front of the molecular clouds. In this case, the nebulae should be density bounded in our direction, which implies that an important fraction of the ionizing photons of these H II regions are lost to the diffuse interstellar medium. This result is in agreement with Reynolds (1984, 1990) who, based on the Hα flux of the ionized diffuse regions of the Galaxy, estimates that about 20% of the ionizing photons are lost by H II regions into the low density interstellar medium.

The presence of a wind-driven bubble or co-moving H I, molecular/H II large scale sheets (as suggested by Meaburn 1977) are unlikely to be the dominant kinematic structures in these H II regions because they do not predict a velocity-ionization potential stratification in the nebulae (see Meaburn & Walsh 1981). In fact, both scenarios predict that all the emitting gas is moving at the same velocity; i.e. in these cases, we would measure the same velocity for all ionic species. Moreover, spectroscopic studies with higher spectral resolution have shown that the presence of spherically expanding or "academic" bubbles is unlikely, due to the absence of systematic centre-to-edge velocity variation in the line profiles (e.g. Hänel 1987).

The flows from the ionization front in the back of the H II region is not the only source available to explain the velocity pattern close to the Trapezium stars, and other mechanisms have been considered, such as mass loss from θ^1C, θ^1D, and θ^2A Orionis (e.g. Snow & Morton 1976; Taylor & Münch 1978; Franco & Savage 1982). Franco & Savage (1982) have found that θ^1C Ori, the hotest star of the Trapezium, exhibits interstellar absorption lines both of a low degree of ionization, such as those of C I, N I, O I, and Mg I, and of a high degree of ionization, such as those of C IV and Si IV, with a radial velocity behaviour similar to that of the emission lines in the sense that the lines of higher ionization degree are blueshifted relative to those of lower degree of ionization. These observations imply that the material closer to the star, which has a higher degree of ionization and is farther away from us, is blueshifted with respect to the material closer to us, which has a lower degree of ionization, exactly the oposite of the idea of Zuckerman (1973), Balick et al. (1974) and many others that the lines of low degree of ionization originate behind the Trapezium stars and not in front. This apparent paradox might be solved in the following way: a) the mass loss rate of θ^1C Ori is small and only affects the region where the C IV and Si IV lines are formed, b) the Orion nebula is ionization bounded, at least in the line of sight between us and θ^1C Ori, and the absorption lines of low degree of ionization originate in a neutral region that has not yet been affected by the H II region gas flows and consequently have velocities similar to those of the molecular cloud. To summarize this discussion and considering the similar relation between the ionization potential and the radial velocities of M 8, M 17, and M 42 it follows that mass loss from stars in these nebulae are not responsible for the main features of the velocity field.

Assuming the flows of ionized gas from ionization fronts as the most probable scenario, the different behaviour of the velocity-ionization potential relation found between the slit positions observed can be understood by means of geometrical considerations. Models by Meaburn (1975) and Elliott & Meaburn (1975b) predict that velocities of the ionized gas similar to the neutral or molecular clouds can be identified with gas flows streaming tangentially away from the molecular cloud; in contrast, lower velocities in the ionized gas are observed from flows oriented towards the observer. If we consider different inclination angles between the face of the molecular cloud and our line of sight, we would have different velocity separations between the ionized and neutral or molecular gas. Also, different combinations of: a) distance from the ionizing star to the ionization front; b) structure of the surface of the ionization front; c) density structure or stratification inside the nebula; all are factors that could affect the precise shape of the velocity-ionization potential stratification we are observing in a given line of sight.

5. Conclusions

In this paper we present heliocentric velocities for an unprecedently large number of ionic species in two slit positions of the Galactic H II regions M 42 and M 17 and one slit position of M 8. The range of ionization potential covered goes from neutral species to Ne III (41 eV).

The behaviour of the velocity-ionization potential relation of the ions in all the H II regions observed is fairly similar, with a general decrease of the heliocentric velocity with the ionization energy. This indicates that the spatial stratification of velocities of the ionized gas should be similar in the three objects.

After discussing several possibilities, we conclude that the picture of flows of ionized gas streaming away from the molec-

ular cloud towards the observer is the most suitable scenario to explain the observations. Finally, the observed velocity vs. ionization degree structure for these three H II regions also indicates that they should be density bounded in the direction towards the observer, providing a source of ionizing photons for the low density interstellar medium.

Acknowledgements. We are grateful to Jorge García-Rojas for his help in reducing part of the data for M 8 and Elysandra Figueredo for the fitting of part of the emission lines of M 42. We thank the referee, M. Bautista, for his valuable comments. CE would like to thank all the members of the Instituto de Astronomía, UNAM, for their warm hospitality during his stays in Mexico. This research was partially funded though grant no. PB94-1108 from the Dirección General de Investigación Científica y Técnica of the Spanish Ministerio de Educación y Ciencia.

References

Baldwin J.A., Crotts A., Dufour R.J., et al., 1996, ApJ 468, L115
Balick B., Gammon R.H., Hjellming R.M., 1974, PASP 86, 616
Bautista M.A., Pradhan A.K., 1995, ApJ 442, L65
Bautista M.A., Pradhan A.K., 1998, ApJ 492, 650
Castañeda H.O., 1988, ApJS 67, 93
Clayton C.A., Ivchenko V.N., Meaburn J., Walsh J.R., 1985, MNRAS 216, 761
Dopita M.A., 1972, A&A 17, 165
Elliott K.H., Goudis C., Hippelein H., Meaburn J., 1984, A&A 138, 451
Elliott K.H., Meaburn J., 1975a, MNRAS 172, 427
Elliott K.H., Meaburn J., 1975b, Ap&SS 35, 81
Elliott K.H., Meaburn J., Terret D.L., 1978, MNRAS 184, 527
Esteban C., Peimbert M., Torres-Peimbert S., 1999a, A&A 494, L37
Esteban C., Peimbert M., Torres-Peimbert S., Escalante V., 1998, MNRAS 295, 401
Esteban C., Peimbert M., Torres-Peimbert S., García-Rojas J., 1999c, Rev. Mex. Astron. Astrofis. 35, 65
Esteban C., Peimbert M., Torres-Peimbert S., García-Rojas J., Rodríguez M., 1999b, ApJS 120, 113
Fehrenbach Ch., 1977, A&AS 29, 71
Franco J., Savage B.D., 1982, ApJ 255, 541
Goudis C., 1982, The Orion Complex: A Case Study of Interstellar Matter. Reidel, Dordrecht
Goudis C., Meaburn J., 1976, A&A 51, 401
Hänel A., 1987 A&A 176, 338
Kaler J.B., 1967, ApJ 148, 925
Kaler J.B., Aller L.H., Bowen I.S., 1965, ApJ 141, 912
Lada C.J., Dickinson D.F., Penfield H., 1974, ApJ 189, L35
Lada C.J., Gull T.R., Gottlieb C.A., Gottlieb E.W., 1976, ApJ 203, 159
Meaburn J., 1975, Ap&SS 35, L5
Meaburn J., 1977, In: Van Woerden H.D. (ed.) Topics in Interstellar Matter. Reidel, Dordrecht, 81
Meaburn J., Walsh J.R., 1981, Ap&SS 74, 169
O'Dell C.R., Wen Z., 1992, ApJ 387, 229
Reynolds R.J., 1984, ApJ 282, 191
Reynolds R.J., 1990, In: Bloeman H. (ed.) IAU Symp. 144, The Interstellar Disk/Halo Connection in Galaxies. Kluwer, Dordrecht, 67
Snow T.P., Morton D.C., 1976, ApJS 32, 429
Taylor K., Münch G., 1978, A&A 70, 359
Wen Z., O'Dell C.R., 1993, ApJ 409, 262
Wilson O.C., Münch G., Flather E., Coffeen M.F., 1959, ApJS 4, 199
Wright E.L., Lada C.J., Fazio G.G., Kleinmann D.E., 1977, AJ 82, 132
Zuckerman B., 1973, ApJ 183, 863